

# Page image classifier fine-tuned on century-spanning archives of scanned documents for further content-specific processing

Kateryna Lutsai [ORCID:0009-0002-4773-2797](#)<sup>1\*</sup>, Dana Křivánková [ORCID:0000-0001-5718-9447](#)<sup>2</sup>, David Novák [ORCID:0009-0005-8722-0245](#)<sup>3†</sup>, Pavel Straňák [ORCID:0000-0002-6895-8536](#)<sup>4†</sup>

<sup>1,2</sup>Institute of Formal and Applied Linguistics, Charles University MFF, Malostranské náměstí, Prague, 11800, Czech Republic.

<sup>3</sup>Institute of Archaeology, Czech Academy of Sciences, Letenská, Prague, 11800, Czech Republic.

\*Corresponding author(s). E-mail(s): [lutsai@ufal.mff.cuni.cz](mailto:lutsai@ufal.mff.cuni.cz);  
Contributing authors: [krivankova@arup.cas.cz](mailto:krivankova@arup.cas.cz); [novak@arup.cas.cz](mailto:novak@arup.cas.cz);  
[stranak@ufal.mff.cuni.cz](mailto:stranak@ufal.mff.cuni.cz);

<sup>†</sup>These authors contributed equally to this work.

## Abstract

**Purpose:** Digitization projects in the humanities produce vast, heterogeneous archives of historical documents, making manual sorting impractical at scale. This work addresses the need for an automated system to classify scanned page images based on visual content type — text, tables, and graphics — enabling content-specific downstream processing such as Optical Character Recognition (OCR) or structured data extraction.

**Methods:** An image classification system was developed and evaluated on a dataset of over 48,000 annotated historical page images from century-old Czech archaeological archives, refined through four successive annotation stages with domain-expert review. A Random Forest Classifier baseline was established using hand-crafted image features. Subsequently, deep learning architectures were fine-tuned and compared: Convolutional Neural Networks (EfficientNetV2, RegNetY), Vision and Document Image Transformers (ViT, DiT), and multimodal CLIP models. An 11-category label scheme was designed collaboratively with domain experts and evaluated via five-fold cross-validation.

**Results:** The feature-based baseline achieved approximately 75% accuracy. Fine-tuned CNNs and Transformers substantially outperformed it, with RegNetY-16GF achieving 99.16% and ViT-large 99.12% Top-1 accuracy on the held-out test set. CLIP ViT-B/16 reached 99.14% with optimized text descriptions.

**Conclusion:** Image-only models, particularly RegNetY-16GF, deliver near-perfect classification accuracy and produce consistent labels across 649,508 unlabeled archival pages with over 90% inter-model agreement. Fine-tuned CLIP, despite competitive test-set accuracy, showed under 65% agreement with image-only models on unlabeled data, making it less suitable for deployment. The final models, annotated dataset, and software are publicly available under open-source licenses.

**Keywords:** Image-based Document Processing, Archival Digitization, Page classification, Historical document image analysis, Vision Transformers

# 1 Introduction

The spread of large-scale digitization initiatives in libraries, archives, and museums has generated massive digital collections of historical documents. For a long time, paper materials and digitization workflows were the foundation of both newly created and old document collections, until archived documents became digital-born. While digitization of paper materials significantly improves accessibility, the management and analysis of these vast, complex repositories presents considerable challenges.

Digital archives derived from historical documents exhibit several unique characteristics that complicate their management. The collections often span significant historical periods, with document creation ranging from the early 20th century to the present day, and the data volume typically increases exponentially over time, as illustrated in Fig. 1. The archive studied here spans roughly a century (approximately 1920–2020); the “century-old” framing in the title refers to its earliest material, while the bulk of the collection is more recent, as Fig. 1 makes clear. High-resolution scanning results in large image files, and the physical condition of original documents can introduce visual defects into scans.

Furthermore, these archives are marked by profound heterogeneity. A single collection can contain a wide variety of content types, often combined within a single document. As demonstrated in Figs. 2 and 3, this includes everything from handwritten manuscripts and typed correspondence to printed articles, technical drawings, maps, and photographs.

In addition, scanned documents frequently suffer from metadata scarcity. File names often encode technical details, such as the scan date, rather than semantic content. Critical information like author, title, or language is often missing, complicating automated processing. This combination of diversity and poor documentation is a well-known characteristic of large-scale digitization efforts [1].

The characteristics outlined above create significant hurdles for effective archive management:

**Sorting and Organization:** The sheer volume and heterogeneity make manual sorting impractical. Scanning campaigns often generate large

batches, raising the risk of human error. Processing documents with default equipment settings leads to absent descriptive metadata (language, document type, collection), preventing straightforward automated grouping.

**Manual Processing Time:** Manually reviewing each page to determine its content category is prohibitively time-consuming and unsustainable at scale, a widely recognized challenge in digital humanities [1].

**Need for Content-Specific Processing:** Different page types require different tools; Optical Character Recognition (OCR) is appropriate for text, layout analysis for tables [2, 3], and image segmentation for photographs. Without an initial classification step, these downstream pipelines cannot be applied efficiently.

Initial consultations with the data providers confirmed that the collection was perceived as highly disorganized, reflecting a common reality where the scale of data acquisition outstrips the resources available for curation.

To address these challenges, this research develops an automated system for classifying page images from historical archives based on their visual content and layout. The primary contribution is the implementation and rigorous evaluation of multiple classification approaches — from classical feature-based methods to state-of-the-art deep learning networks — on a unique, large-scale real-world archival collection. A detailed description of all experiments and implementation details is available in the accompanying thesis [4].

*LLM use disclosure.* This manuscript was prepared with assistance from large language models (Gemini 2.5, GPT-4) for text drafting and generation from author-supplied bullet-point outlines, as well as for copy editing (style, grammar, and formatting). All generated content was reviewed, verified, and revised by the authors, who take full accountability for the final text. Full details are provided in the disclosure at the end of this article.

The remainder of this article is organized as follows. Section 2 reviews prior work. Section 3 provides a detailed overview of the raw data and its properties. Section 4 describes the classification methodology. In Sect. 4.3, the proposed system architecture is detailed. Section 5 presents performance results and practical integration. Section 5.3 analyses prediction agreement on the

**Fig. 1** Number of page scans over time (the overall collection of unlabeled source files)

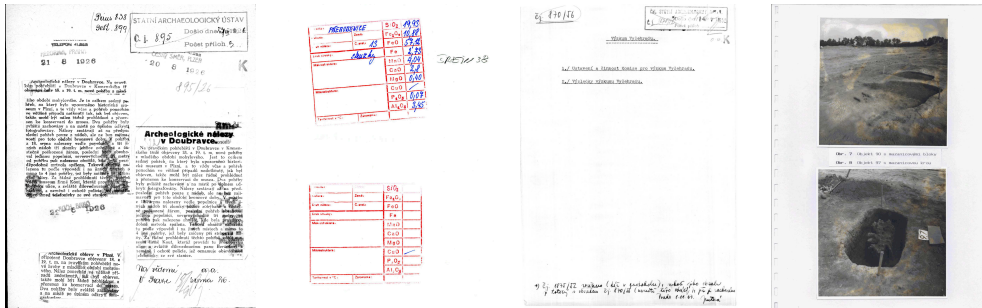
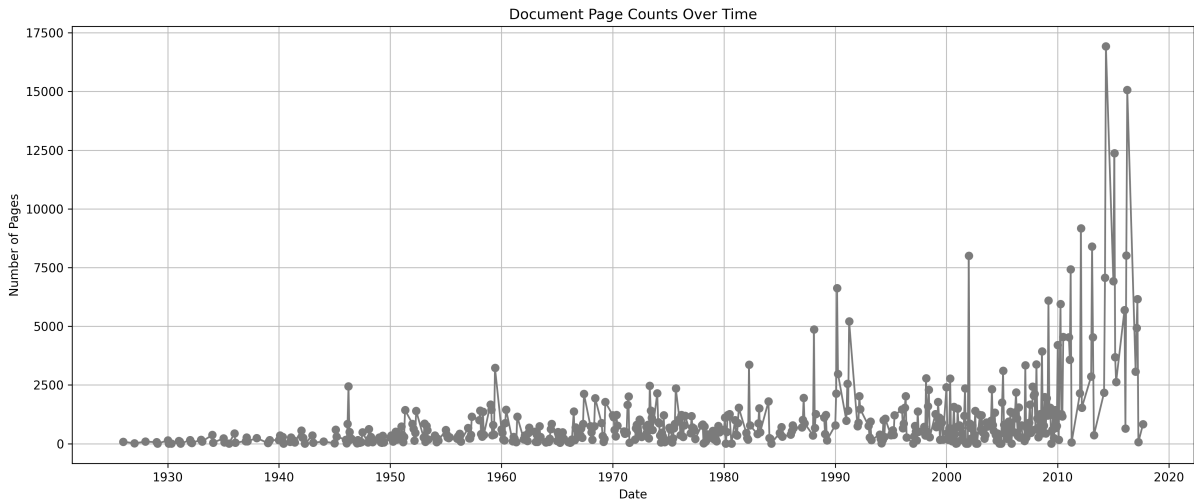


**Fig. 2** Samples of various page types from the archive

full unlabeled collection. Finally, Sect. 6 concludes the paper.

## 2 Background and Related Work

### 2.1 Document Image Classification

Document image classification has been studied for several decades. Early work established standard benchmarks and demonstrated the utility of convolutional architectures. Lewis et al. [5] constructed the IIT-CDIP collection of 42 million scanned tobacco-industry documents, which became the standard pre-training corpus for document-specific models. The RVL-CDIP benchmark [6], derived from IIT-CDIP, contains 400,000 grayscale document images across 16 categories (letters, memos, forms, invoices, etc.) and has

since served as the primary evaluation standard for document image classification. Initial approaches relied on hand-crafted features and classical classifiers; the survey by Liu et al. [7] traces the progression from these methods to deep convolutional networks and documents the steady accuracy gains over two decades of work.

A comprehensive survey by Nikolaidou et al. [1] covering historical document image datasets reports that, despite the richness of available corpora, most datasets originate from well-preserved, printed Western European sources and focus on text recognition rather than holistic page-level classification. The challenge of managing genuinely heterogeneous archives — spanning handwriting, photographs, maps, and forms across more than a century — is largely unaddressed by existing benchmarks.

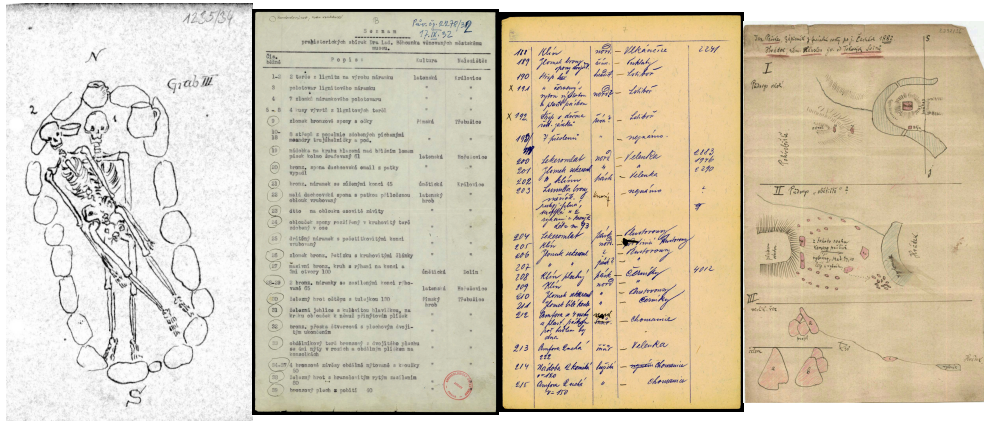


Fig. 3 Samples of various page types from the same collection, showing diversity in size, content, and condition

## 2.2 Deep Learning Architectures for Document Analysis

Convolutional neural networks have proven highly effective for document image classification. Harley et al. [6] showed that CNNs substantially outperform hand-crafted features on RVL-CDIP, establishing the template for subsequent fine-tuning approaches. The EfficientNetV2 family [8, 9] and RegNet design spaces [10] offer accuracy-efficiency trade-offs well suited to large-scale batch processing: smaller variants run on standard CPUs, while larger ones match or exceed Transformer accuracy at lower computational cost.

Vision Transformers (Vision Transformer (ViT) [11, 12]) and their distillation variants [13] have achieved top-tier results on ImageNet [14] and transfer competitively to document tasks when pre-trained on large corpora. The Document Image Transformer (DiT) [15] extended this paradigm by pre-training directly on IIT-CDIP via BEiT-style masked image modelling, reaching state-of-the-art performance on RVL-CDIP without any convolutional inductive biases.

Document layout analysis and structure understanding received further impetus from multimodal models. LayoutLM [3] jointly models textual content and spatial layout from OCR-extracted tokens, achieving strong results on form understanding and information extraction benchmarks. However, LayoutLM and its successors require reliable OCR output — a prerequisite that fails on the noisy, handwritten, and structurally degraded pages common in historical archives.

## 2.3 Multimodal and Zero-Shot Classification

Contrastive Language-Image Pretraining (CLIP) [16], pre-trained by aligning images and their natural-language captions on 400 million web image-text pairs [17], enables zero-shot image classification by scoring similarity between an image and textual category descriptions. This property is attractive for document classification, where categories can be described in natural language without requiring labeled images. However, zero-shot CLIP is known to underperform on domain-specific or fine-grained visual tasks, where the pre-training distribution diverges from the target [7]. Fine-tuning recovers much of this gap, as we demonstrate in Section 4.2.4.

## 2.4 Historical Document Analysis

Historical document archives present additional challenges beyond those in standard benchmarks: physical degradation (yellowing, stains, tears), mixed content within a single page, metadata scarcity, and extreme temporal heterogeneity spanning a century of visual styles [1]. Prior work on historical document processing has focused predominantly on handwriting recognition and text line segmentation rather than holistic page-level classification [1]. The present work fills this gap by developing a domain-specific label taxonomy and a large annotated dataset targeting the heterogeneous page-level characteristics of a real-world archaeological archive.

### 3 Exploration of the Raw Data

The primary dataset consists of scanned pages from the Institute of Archaeology of the Czech Academy of Sciences in Prague (Archeologický ústav AV ČR Praha v. v. i. (ARÚP), IAP) (primary source) and Institute of Archaeology of the Czech Academy of Sciences in Brno (Archeologický ústav AV ČR Brno v. v. i. (ARÚB), IAB) (secondary source), initially provided as multi-page PDF (Portable Document File) documents. These were converted into individual PNG (Portable Network Graphics) image files, organized into directories corresponding to source documents. The initial data processing and exploration revealed several key characteristics of the collection.

The archive totals approximately 400–420 GB across more than 60,000 PDFs and nearly 650,000 pages, with document creation dates spanning roughly 1920–2020. A parallel processing workflow was established on a computing cluster to convert the PDF files into page-specific images. Large-format scans occasionally led to truncated images; these were re-processed with greater memory allocation. Following conversion, single-page documents were consolidated into a common folder, and original PDF files were removed to conserve storage. This image-based dataset then formed the basis for exploratory analysis and manual annotation.

#### 3.1 Characteristics of the Source Data

##### 3.1.1 Visual Defects of the Scanned Pages

The scanned pages frequently exhibited visual defects originating from the physical condition of source documents and the scanning process itself. These artifacts range from minor blemishes to severe degradation that complicates automated content extraction. Representative examples of each defect type are provided in Online Resource 1. The primary defect categories are as follows.

- **Background Artifacts and Low Contrast:** Aged, yellowed, or gray paper backgrounds diminish contrast between text and page (Fig. 3; Online Resource 1).
- **Page Skew and Alignment Issues:** Many pages suffer from skew, where content is not aligned horizontally (Online Resource 1). This is a well-documented problem in OCR literature [18] that often requires specialized pre-processing to correct.
- **Text Bleed-Through:** On thin paper, ink from the reverse side is visible, creating superimposed text that interferes with primary content (Online Resource 1).
- **Water Damage:** Some documents show water damage resulting in blurred ink, stains, and overlapping text (Online Resource 1).
- **Physical Damage:** Prevalent physical damage includes tears, holes, and worn edges (Online Resource 1). This ranges from corner tears to significant edge damage and binding punch holes.
- **Stamps and Annotations:** Official stamps and ink annotations are frequently found, sometimes appearing as faint graphical elements (Online Resource 1). Only fillable stamps are of interest since they are processed as tabular data.
- **Scanning Artifacts from Bound Volumes:** Scanning from thick bound journals introduces page curl and a dark gradient near the inner margin (Online Resource 1).
- **Mixed Content:** Pages rarely contain a single content type; mixed layouts combining printed tables, handwritten notes, and drawings are common (Online Resource 1).
- **Manual Corrections:** Crossed-out words, removed paragraphs, and interlinear additions are common throughout the collection (Online Resource 1).

These complex and overlapping defects make naive document processing unreliable, underscoring the need for specialized classifiers robust to visual noise.

##### 3.1.2 Textual Variations and Annotations

Beyond physical defects, the documents displayed considerable heterogeneity in text presentation and annotation. Pages frequently combined multiple text formats — for instance, typed documents with handwritten page numbers or comments (Online Resource 3). Textual elements were commonly embedded within graphical content; maps

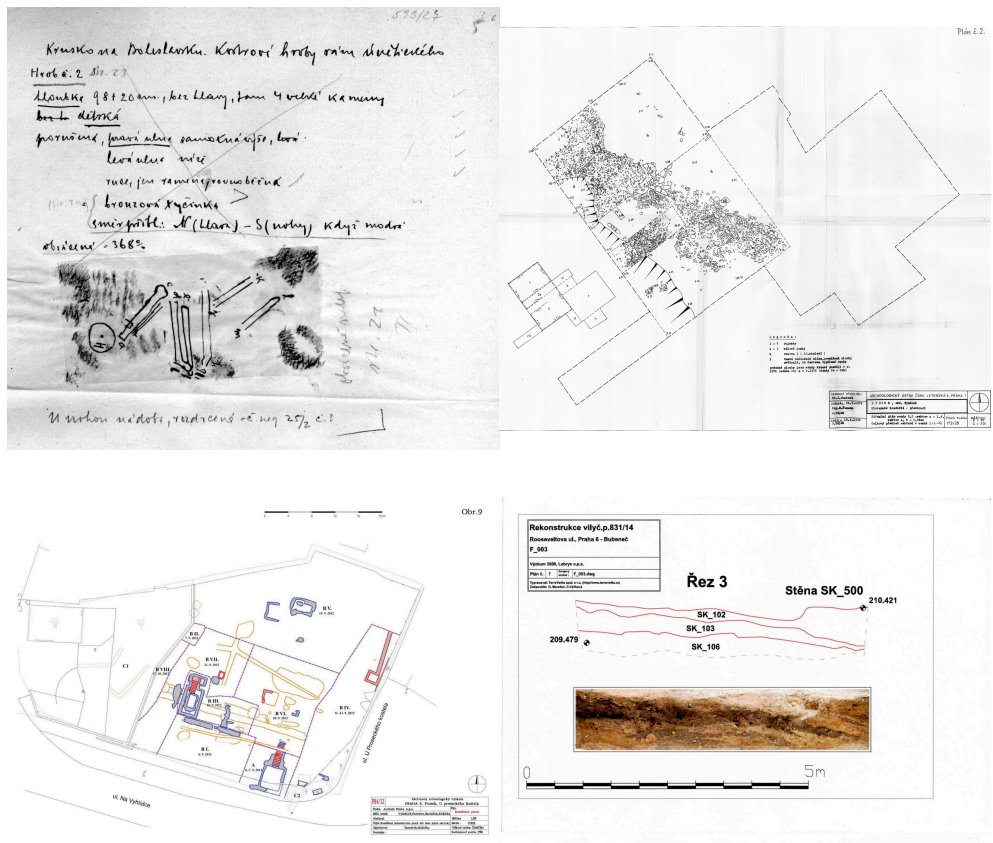


Fig. 4 Samples of pages from different time periods; the newer page on the right is digital-born, yet was scanned for archiving

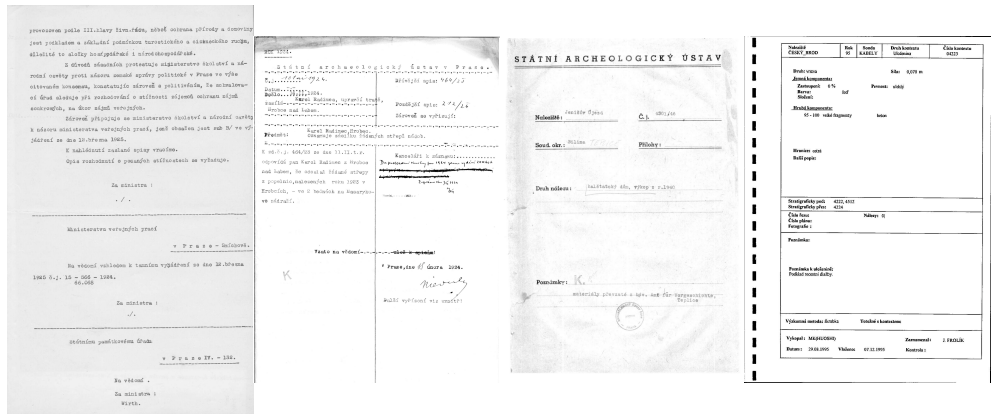


Fig. 5 Samples of pages with complex layouts that degrade standard OCR performance

and drawings included labels and captions, while photographs were often accompanied by typed or handwritten descriptions (Online Resource 3). Consequently, purely graphical pages devoid of any text were relatively rare.

## 4 Methods

### 4.1 Preliminary Analysis and Justification

To establish a performance baseline, an initial analysis was conducted using the [DeepDoctection](#) Document Layout Analysis (DLA) framework and the Tesseract OCR engine [19]. These experiments revealed that off-the-shelf tools were insufficient for the project’s goals. OCR performance degraded substantially on pages with noisy backgrounds (Online Resource 2), structured data detection was unreliable with frequent misclassification of tables (Online Resource 2), and graphical element detection was often inaccurate (Online Resource 2).

For DLA and table recognition, Detectron2 was used under the hood of DeepDoctection (DD)’s table recognition module. Table detection was unreliable: DD often merged rows or missed cells when borders were faint, incomplete, or skewed (Online Resource 2). Maps were sometimes classified as tables, and handwritten annotations on drawings further confused the detector (Online Resource 2).

Feedback from a domain expert at IAP confirmed that out-of-the-box DLA performance was inadequate. Collaboration with the domain expert established a clear set of criteria for page classification, finalized through evaluation on a held-out set of documents:

- **Classification Consistency:** Pages with similar content must receive the same category. Consistency was prioritized over isolated correctness.
- **Primacy of Structured Data:** Pages containing tabular or form-like data must be classified as such, even when significant plain text is also present.
- **Priority of Graphical Content:** A significant graphical element (at least stamp-sized) should take precedence over textual content in determining page category.
- **Handling of Handwritten Annotations:** Minor peripheral notes (e.g., page numbers) may be ignored; central or prominent handwritten elements should influence classification.

- **Robustness to Defects:** The system must be robust to background noise and paper degradation, which caused DD to detect numerous spurious tables and figures (Online Resource 2).

This expert input finalized the category definitions and annotation guidelines. The first set of categories proposed by the data providers is described in Table 1.

### 4.2 Supervised Image Classification Models

Given the limitations of unsupervised DLA methods on heterogeneous historical document data, our focus shifted to supervised image classification. This section details the evolution of classification categories, the development of a baseline low-compute model, the evaluation of state-of-the-art deep learning architectures, and the iterative data refinement that was crucial for achieving high accuracy.

Initially, the categories were defined based on the capabilities of the DLA framework we first tested (Table 1). We then adjusted this scheme to better align with the capabilities of statistical models, noting that a distinction between handwritten and other text types was a promising direction. This led to a proposed set of 7 refined categories (Table 2).

After demonstrating initial results with these categories, the data providers agreed to expand the label set. Following expert feedback, the PHOTO\_TEXT category was replaced by PHOTO\_L and DRAW\_L to better distinguish graphical content in tabular layouts, and the TEXT and TEXT\_LINES categories were subdivided into handwritten (\_HW), machine-typed (\_T), and printed (\_P) variants.

This collaborative process ultimately produced a final set of 11 distinct categories (Table 3). Category-specific temporal characteristics of the final annotation are plotted in Fig. 6. Figure 6 also reveals a gap around the 1990s, when printed monospaced fonts became visually indistinguishable from typewritten text. Pages from this period were not removed from the source collection; rather, they were left unannotated and thus excluded from the ground truth, letting the models infer the distinction on their own. Because these pages were never assigned a label, they are not enumerated in the annotation counts of

Category	Description
REST	Mixture of printed, handwritten, and/or typed text, potentially with minor graphical elements (contained all ambiguous cases).
TEXT.LINE	Pages primarily consisting of machine-typed, printed, or handwritten text organized in a tabular or form-like structure.
PHOTO	Pages dominated by photographs or photographic cutouts (including maps, paintings, schematics) with few text captions.
PHOTO.TEXT	Similar to PHOTO, but the visual content is presented with a text block of any style.
TEXT	Pages containing plain corpora of almost pure printed, handwritten, or typed text.
TEXT.OTHER	Pages containing mixtures of printed, handwritten, and/or typed text, potentially with minor graphical elements.

**Table 1** Overview of categories initially proposed by the data provider

Category	Description
DRAW.TEXT	Pages dominated by drawings, maps, paintings, schematics, or graphics with text labels.
TEXT.LINE	Pages primarily consisting of machine-typed, printed, or handwritten text organized in a tabular or form-like structure.
PHOTO	Pages dominated by drawings, maps, paintings, schematics, graphics, photographs, or photographic cutouts, with few text captions.
PHOTO.TEXT	Similar to PHOTO, but with a significant text block.
TEXT	Pages containing plain corpora of almost pure printed or typewritten text.
HW	Pages consisting purely of handwritten text in paragraph or block form (non-tabular).
TEXT.HW	Pages containing mixtures of handwritten and typed text, potentially with minor graphical elements.

**Table 2** Overview of categories as modifications of the initial ones

Table 5 and appear only as the visible trough around 1990 in Fig. 6.

#### 4.2.1 Classification Categories and Priorities

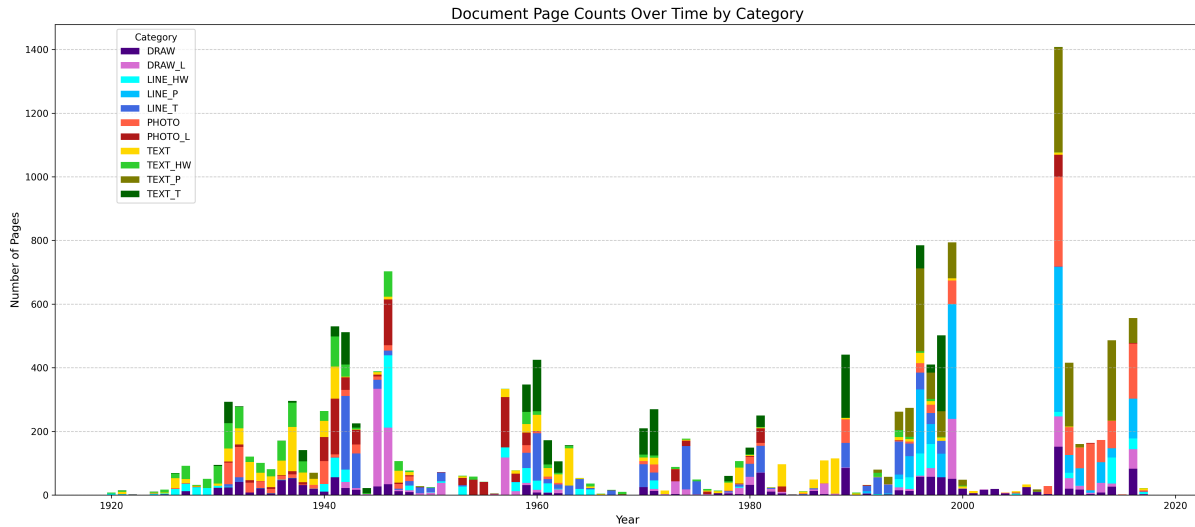
The 11 target classes (Table 3) cover almost half of all content type combinations (Table 12 versus Table 13 in Appendix B). Visual examples for each category are provided in Online Resource 3. Annotation was carried out jointly by the first author and a domain-expert end-user from IAP, using the priority order below as the shared annotation guideline.

A priority order was established to handle pages potentially fitting multiple categories:

1. PHOTOS (PHOTO, PHOTO.L): Highest priority for graphic extraction.
2. DRAWs (DRAW, DRAW.L): Second priority for graphic extraction.
3. LINEs (LINE.HW, LINE.P, LINE.T): Third priority for structured data extraction.
4. TEXTs (TEXT, TEXT.HW, TEXT.P, TEXT.T): Lowest priority, targeting font-specific OCR.

To capture the full variability of the data, we also created an expanded label scheme of 24 distinct types by separating each core category into printed, typewritten, and handwritten variants (Table 13). This comprehensive set was used for analytical purposes, while the 11-category set was used for training the final models.

**Fig. 6** Distribution of categories based on document creation year (final annotated training dataset)



Category	Description
DRAW	Pages dominated by drawings, maps, paintings, schematics, or graphics, potentially containing text labels or captions.
DRAW_L	Similar to DRAW, but the graphical element is presented within a table-like layout or includes a legend formatted as a table.
LINE_HW	Pages primarily consisting of handwritten text organized in a tabular or form-like structure.
LINE_P	Pages primarily consisting of printed text organized in a tabular or form-like structure.
LINE_T	Pages primarily consisting of machine-typed text organized in a tabular or form-like structure.
PHOTO	Pages dominated by photographs or photographic cutouts, potentially with text captions.
PHOTO_L	Similar to PHOTO, but the photograph is presented within a table-like layout or accompanied by tabular annotations.
TEXT	Pages containing mixtures of printed, handwritten, and/or typed text, potentially with minor graphical elements.
TEXT_HW	Pages consisting purely of handwritten text in paragraph or block form (non-tabular).
TEXT_P	Pages consisting purely of printed text in paragraph or block form (non-tabular).
TEXT_T	Pages consisting purely of machine-typed text in paragraph or block form (non-tabular).

**Table 3** Overview of categories used in the trained models

**Annotation reliability.**

The ground truth was produced by two annotators — the first author and a domain-expert end-user from IAP (Ing. Dana Křivánková, the fourth author) — under the oversight of the project lead

(Mgr. David Novák, Ph.D.). Annotation followed an iterative, expert-reviewed protocol: the first author labelled batches that the domain expert then reviewed and approved, and the label disagreements surfaced in this loop directly drove the

evolution of the scheme from 6 to 7 to the final 11 categories (Tables 1–3). The fixed priority rule above (graphics > structured data > text) was the shared mechanism for resolving multi-content pages to a single label. Because every page ultimately carries one adjudicated consensus label, a conventional inter-annotator agreement coefficient is not defined over the full released dataset, and we did not compute a formal Cohen’s  $\kappa$ ; the authors’ qualitative impression is that batch-level agreement improved from roughly  $\kappa \approx 0.5$  early in the project to  $\kappa \approx 0.9$  once the taxonomy and guidelines stabilized. A controlled dual-annotation study on a held-out subset to report a formal  $\kappa$  is left for future work. In the interim, reliability is evidenced indirectly by the explicit priority rules, the iterative expert review across the four dataset versions (Sect. 4.2.5), and the high cross-fold stability and inter-model agreement of the resulting classifiers (Sects. 5.2 and 5.3).

#### 4.2.2 Low-Compute Baseline: Random Forest Classifier

As a computationally efficient baseline, we implemented a traditional computer vision pipeline using a Random Forest Classifier (RFC) [20] requiring no specialized GPUs (Graphics Processing Units). Each image was transformed into a numerical feature vector combining descriptors from grayscale and binarized versions:

- **Preprocessing:** Grayscale conversion, Otsu thresholding [21], and basic image properties (dimensions, pixel ratios).
- **Hu Moments [22]:** Seven invariant moments capturing shape information robust to translation, scale, and rotation.
- **Haralick Texture Features [23]:** Statistics derived from Gray-Level Co-occurrence Matrices (GLCM), describing contrast, correlation, and homogeneity.
- **Histogram Features:** Pixel intensity distributions (256 bins for grayscale, 2 bins for binary).

The resulting 298-float representation enables efficient processing on modest hardware. Several classical classifiers were evaluated on this feature vector — including Latent Dirichlet Analysis (LDA), k-nearest neighbors (k-NN), Naive Bayes, Support Vector Machine (SVM), and logistic regression — with RFC achieving the best

preliminary accuracy, as shown in Fig. 7. The RFC was therefore selected for its efficiency and interpretability. However, this approach achieved only  $\sim 75\%$  accuracy, demonstrating the need for more powerful deep learning models.

At that point, we annotated data according to the data provider suggestions (Table 1) and our own refined propositions (Table 2), then trained the RFC model to demonstrate its performance at the first workshop. Development-set evaluation results are shown in Fig. 8.

#### 4.2.3 Deep Learning Approaches: CNNs and Transformers

We evaluated several deep neural network architectures by fine-tuning models pre-trained on different datasets. All models in Table 4 were fine-tuned with a consistent set of data augmentations, using five-fold cross-validation with an 80%/10%/10% train/development/test split on the final annotated dataset. Image-only models were fine-tuned for 3 epochs per fold; the resulting per-fold checkpoints were subsequently averaged to produce the final deployment weights, following the procedure described in [4].

**Training configuration.** All image-only models were trained using AdamW with a learning rate of  $10^{-5}$ , linear warmup over 10% of training steps, and per-epoch checkpointing with best-model selection based on development-set accuracy. Batch size was set to 12–16 pages depending on available GPU memory. Data augmentation applied randomly and independently per image: brightness, contrast, saturation, and hue adjustments (each at probability 0.5), sharpness scaling (random factor 0.5–1.5), and Gaussian blur (random radius 0–2). Geometric transformations (rotation, flipping) were deliberately excluded to preserve document orientation cues.

- **Convolutional Neural Networks (CNNs) (EfficientNetV2 and RegNetY):** We fine-tuned variants of EfficientNetV2 [8, 9] and RegNetY [10]. The final classification layer was replaced to match our 11 classes. Among EfficientNetV2, the medium variant proved most efficient at 98.83%; RegNetY-16GF emerged as the top overall performer at 99.16%, surpassing its larger 64GF sibling.
- **Vision Transformers (ViT and DiT):** We fine-tuned variants of Vision Transformer

**Fig. 7** Comparison of low-compute classifiers (RFC, LDA, k-NN, SVM, Naive Bayes, logistic regression) on the data-provider scheme (left) and our proposed scheme (right), evaluated via cross-fold validation on fewer than 2,000 images. RFC outperforms all classical alternatives on both label sets

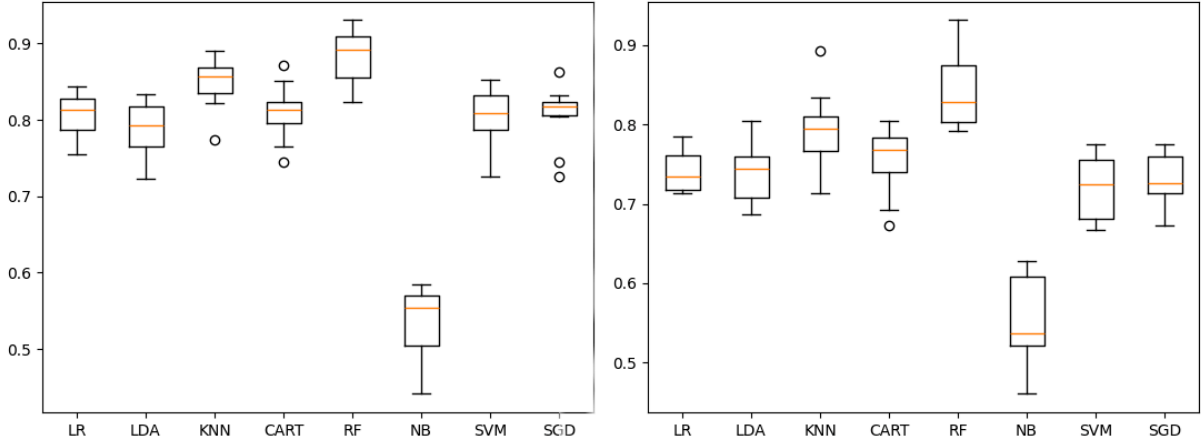
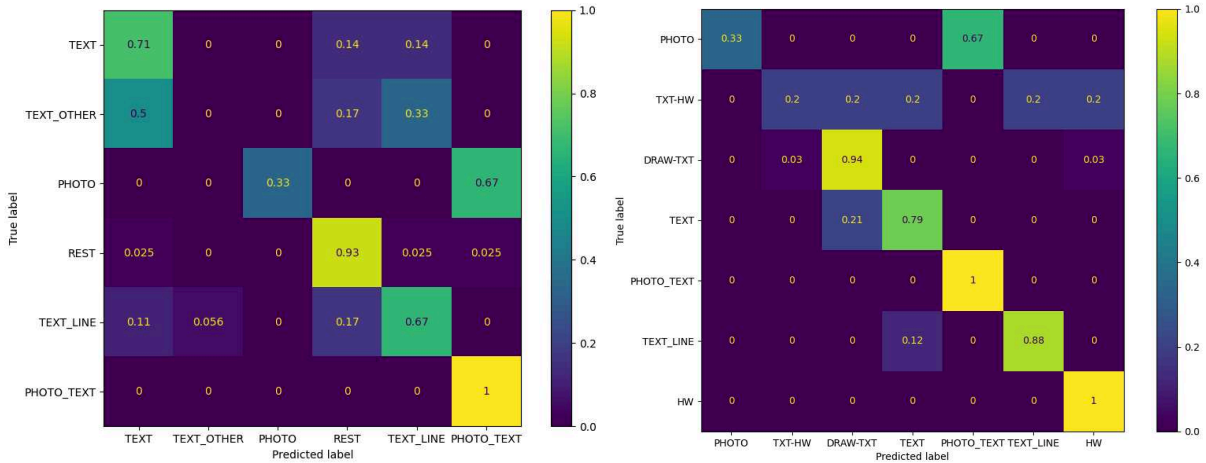


**Fig. 8** RFC experiments on data providers' (left) and ours (right) annotations of fewer than 2,000 images



(ViT) [11, 12] and Document Image Transformer (DiT) [15], the latter pre-trained on large-scale document images from IIT-CDIP [5] and optionally fine-tuned on RVL-CDIP [6]. ViT-large reached  $\approx 99.12\%$  Top-1 accuracy; DiT variants achieved 98–99%, consistent with CNNs but not surpassing the best CNN models.

#### 4.2.4 Multimodal Approach: CLIP

Finally, we investigated a multimodal approach using Contrastive Language-Image Pretraining (CLIP) [16], which learns visual representations from natural language supervision. In contrast to image-only models, CLIP was fine-tuned for 7 epochs with a learning rate of  $5 \times 10^{-5}$  on

the first fold of the cross-validation split. This asymmetric evaluation (one fold rather than five) was a pragmatic choice given the substantially higher computational cost of CLIP fine-tuning; results should therefore be interpreted as indicative rather than fully comparable to the five-fold image-only scores.

The best-performing configuration — CLIP-ViT-B/16 with the *mid* category description set (Table 10) — reached 99.14% accuracy on the held-out test set (Fig. 9), comparable to the best image-only models. The larger ViT-L variants scored approximately 98.97% (see [4] for full confusion matrices of all CLIP variants).

Model	Input Size	Pre-training Dataset	Params (M)
EfficientNet-v2-S	300×300	ImageNet-21k	48.2
EfficientNet-v2-M	384×384	ImageNet-21k & ImageNet-1k	54.1
EfficientNet-v2-L	384×384	ImageNet-21k & ImageNet-1k	118.5
RegNetY-12GF	224×224	ImageNet-12k & ImageNet-1k	51.8
RegNetY-16GF	224×224	ImageNet-12k	83.6
RegNetY-64GF	384×384	SEER & ImageNet-1k	281.4
dit-base-rvldcip	224×224	IIT-CDIP (42M) & RVL-CDIP	86
dit-large	224×224	IIT-CDIP (42M)	304
dit-large-rvldcip	224×224	IIT-CDIP (42M) & RVL-CDIP	304
vit-base-patch16	224×224	ImageNet-21k & ImageNet-1k	86.6
vit-base-patch16	384×384	ImageNet-21k & ImageNet-1k	86.9
vit-large-patch16	384×384	ImageNet-21k & ImageNet-1k	304.7
CLIP-ViT-B/32	224×224	WebImageText (400M)	151
CLIP-ViT-B/16	224×224	WebImageText (400M)	150
CLIP-ViT-L/14	224×224	WebImageText (400M)	428
CLIP-ViT-L/14@336px	336×336	WebImageText (400M)	428

**Table 4** Specifications of all evaluated models

**Category descriptions.** The classification task was tested using predefined sets of categories, each paired with a distinct textual description to guide the CLIP model. A summary of all description sets is given in Table 8 in Appendix A; representative examples are provided in Tables 9 and 10. The full suite of eight description sets, ranging from minimalist to detailed approaches, is reproduced in full in the accompanying thesis [4].

Initial experiments revealed varying error rates across individual description sets, leading to an averaging approach that leverages all descriptions to capture a more generalized category representation. Both zero-shot and fine-tuned results were derived from the precomputed mean of all category descriptions’ text features. Forward-looking implications of CLIP’s real-world deployment behavior are discussed in Sect. 5.3.

#### 4.2.5 Dataset Curation and Refinement

Achieving high accuracy was not just a matter of model selection but also of careful dataset curation. The training data evolved through four successive annotation stages, as summarized in Table 5. We measured the impact of these changes by evaluating a baseline ViT model on each dataset version.

Initially, our annotation set (Dataset 0: 11,940 pages) had limited document variety. We expanded samples within each category, corrected misclassifications, and reclassified ambiguous items like stamps. One iteration, referred to as *poor selection* (Dataset 1), involved removing samples that seemed too noisy or redundant; however, evaluation revealed that removing these distinct examples was detrimental to performance. Consequently, the final annotation phase (Dataset 3: 48,499 pages) involved restoring removed pages to ensure sufficient sample diversity, particularly for the PHOTO, TEXT\_P, and TEXT\_T categories.

The pronounced class imbalance in Dataset 3 is not a design choice but reflects the natural composition of the archive, in which mixed-style plain text (TEXT) and typed tabular pages (LINE\_T) dominate. To prevent the majority TEXT class (14,227 available pages) from overwhelming training and biasing the model against the minority graphical and tabular categories, we capped TEXT at 14,000 pages for the training/development/test partition; the 227 surplus TEXT pages were not discarded but reserved for test-only evaluation, so that measured accuracy on TEXT remains unbiased by the cap. We retained the natural imbalance of the remaining categories and addressed it at training time with a `BalancedBatchSampler`

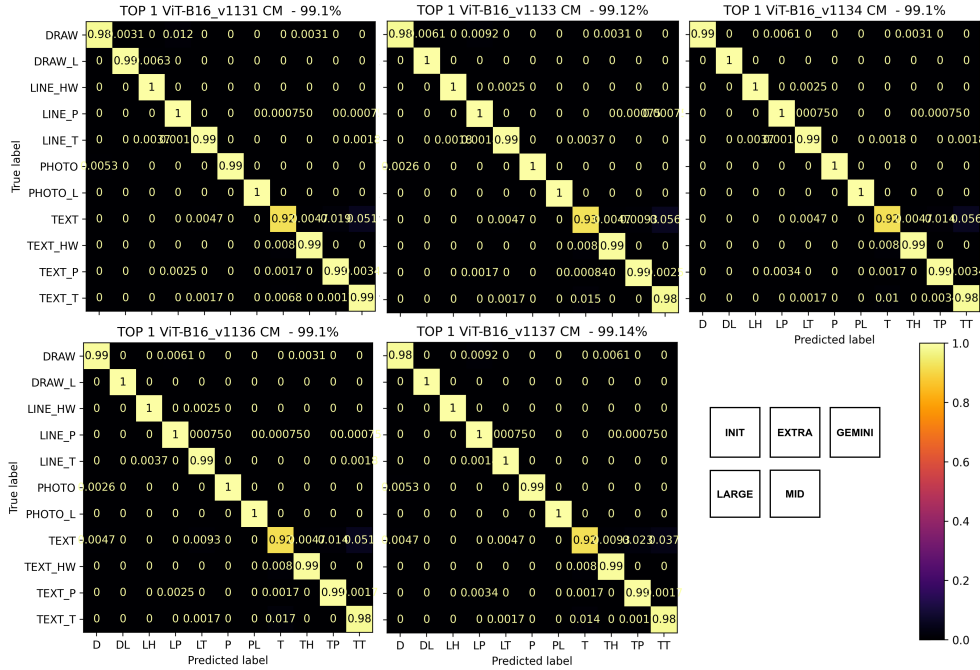


**Fig. 9** Confusion matrix of the best CLIP configuration: ViT-B/16 fine-tuned with the *mid* category description set (Table 10), achieving 99.14% accuracy on the standard test set (5,449 pages)

**Table 5** Category distribution across annotation versions. Datasets 0–2 share the same 11-category scheme but use earlier annotation passes; the full per-category counts for all four versions are listed. The TEXT category was capped at 14,000 samples for training (227 additional TEXT pages were reserved for test evaluation only). Dataset 1 (*poor-selection*) was abandoned after evaluation showed removing noisy-but-distinct pages was detrimental

Category	Dataset 0	Dataset 1	Dataset 2	Dataset 3
DRAW	1,090	1,368	1,472	2,709
DRAW_L	1,091	1,383	1,402	2,921
LINE_HW	1,055	1,113	1,115	2,514
LINE_P	1,092	1,540	1,580	2,439
LINE_T	1,098	1,664	1,668	9,883
PHOTO	1,081	1,632	1,730	2,691
PHOTO_L	1,087	1,087	1,088	2,830
TEXT	1,091	1,587	1,592	14,227
TEXT_HW	1,091	1,092	1,092	2,008
TEXT_P	1,083	1,540	1,633	2,312
TEXT_T	1,081	1,476	1,482	3,965
<b>Unique PDFs</b>	<b>5,001</b>	<b>5,694</b>	<b>5,729</b>	<b>37,328</b>
<b>Total Pages</b>	<b>11,940</b>	<b>15,482</b>	<b>15,854</b>	<b>48,499</b>

(Sect. 4.3) rather than by further sub-sampling, since the *poor-selection* experiment had shown that discarding distinct pages hurts generalization.

Figure 12 shows the Top-1 prediction confusion matrices for ViT-Base trained on the initial, poor-selection, and final dataset versions, illustrating

performance improvements gained through careful data curation. Temporal category distributions across all three annotation versions, revealing the characteristic 1990s gap where printed monospaced fonts were excluded, are provided in Online Resource 4.

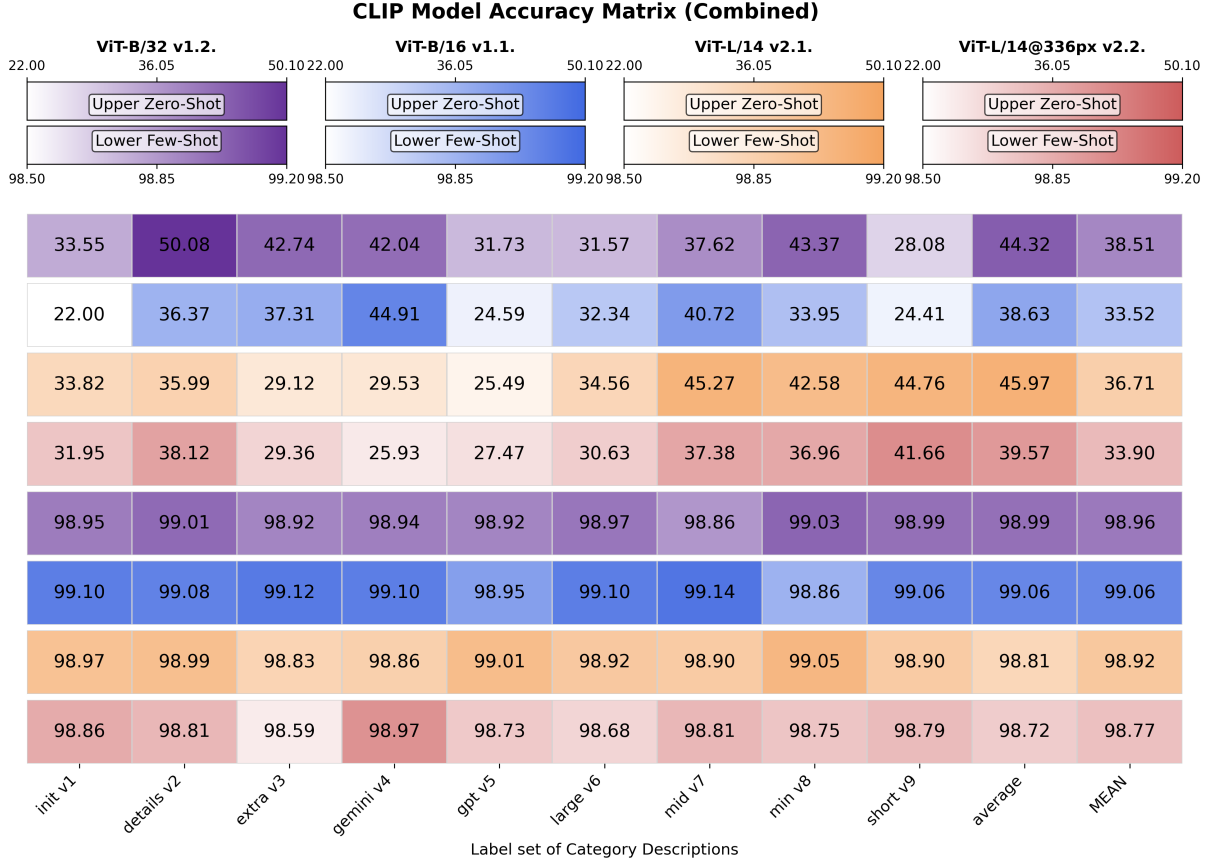


**Fig. 10** Combined zero-shot and fine-tuned CLIP models: comparison of classification accuracy across category description sets on the standard test dataset (5,449 pages)

For the final Dataset 3 models, we used a five-fold cross-validation scheme with an **80%/10%/10%** train/development/test split. For each fold the final subset counts were 38,625 / 4,823 / 4,823 for train/development/test respectively. Rather than a naive random shuffle, a time-aware periodic sampling procedure was employed: for each category, every  $S$ -th element is drawn from the alphabetically (approximately chronologically) ordered sequence, with a bounded random offset, ensuring chronological coverage and reducing the risk of evaluation sets dominated by a single scanning campaign [4]. Consistent category coverage across all five folds is confirmed by Online Resource 4.

Overall, 43,050 images were used across the five training subsets; the remaining 5,449 images formed the final performance test subset used for all model comparisons (Sect. 5.2).

### 4.3 System Architecture and Implementation

The system is implemented as a modular Python application using PyTorch [24] and Hugging Face’s Transformers library [25]. The complete codebase is publicly available in a GitHub repository [26] under the MIT license. The visualization of system architecture for various models is given in Figs. 18 and 19 in Appendix B.

The system offers a Command-line Interface (CLI) (`run.py`) for direct control over operations like training, evaluation, and inference (documented in Table 11 in Appendix B), along with a central configuration file (`config.txt`) for managing parameters such as model selection, learning rates, and input/output paths without code modification.

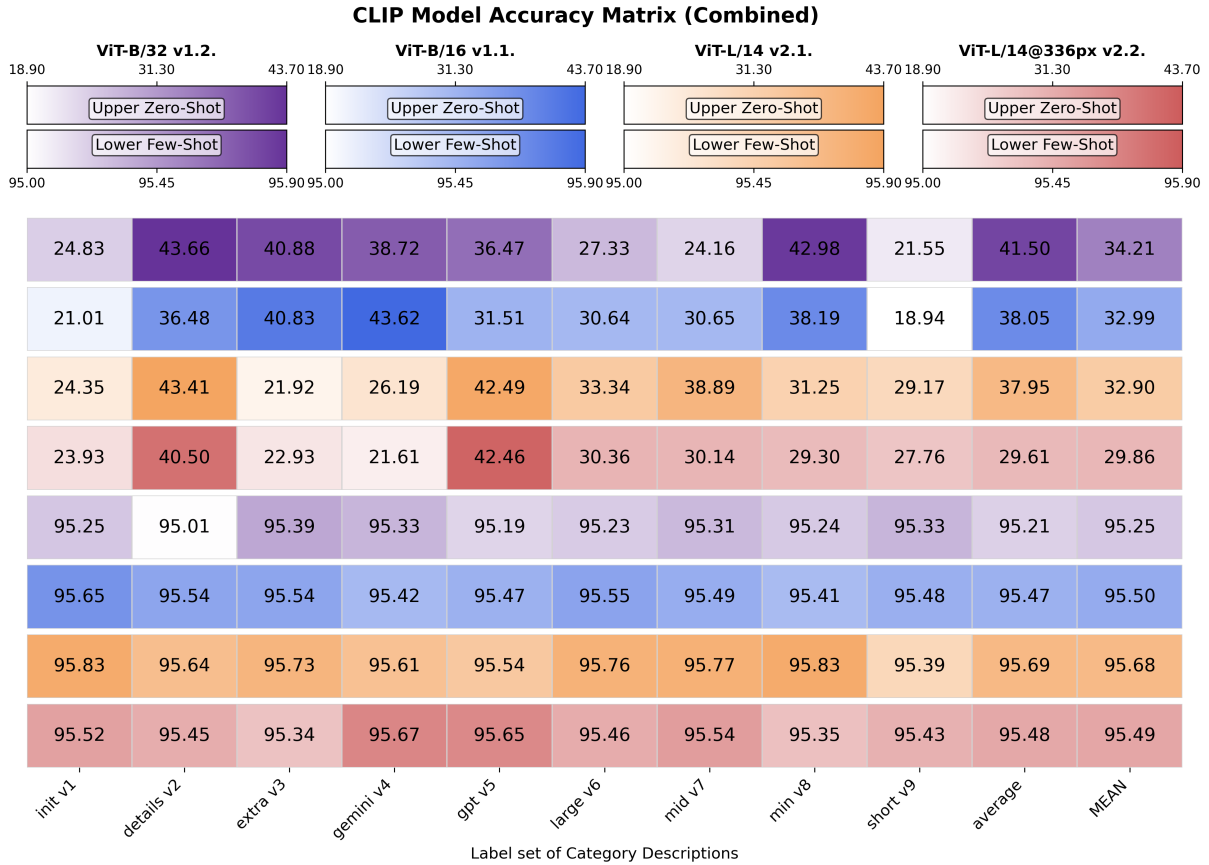


**Fig. 11** Combined zero-shot and fine-tuned CLIP models: comparison of classification accuracy across category description sets on an expanded test dataset (all non-training samples from the first-fold split, random seed 420; 14,162 pages)

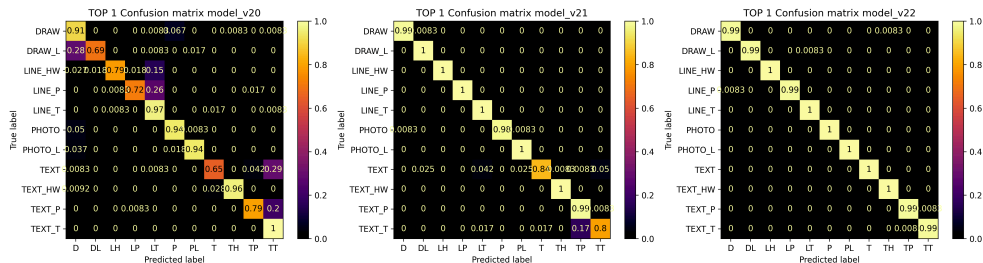


**Fig. 12** Confusion matrices of Top-1 predictions for ViT-Base 224×224 fine-tuned on successive dataset versions. From left to right: Dataset 0 (initial, 11,940 pages), Dataset 1 (poor selection, 15,482 pages), Dataset 3 (final, 48,499 pages)

The system accepts single images or directories of images in standard formats (PNG, JPEG (Joint Photographic Experts Group), etc.). For training, it employs a custom **BalancedBatchSampler** to ensure each batch contains a balanced representation of classes, improving training stability with

imbalanced datasets. Data augmentation (brightness, contrast, saturation adjustments) is applied during training to improve model robustness; geometric transformations are avoided to preserve document layouts. The dataset is split into training (80%), development (10%), and test (10%) sets using stratified sampling.

**Table 6** Configuration settings in `config.txt`

Section	Description
[INPUT]	Specifies the default directory of input images for processing.
[OUTPUT]	Defines paths for result <code>CSV</code> (Comma-separated Values) files, model checkpoints, and visualization outputs.
[SETUP]	Contains operational parameters such as batch size and the value <code>N</code> for top- <code>N</code> predictions.
[TRAIN]	Stores training-specific settings: dataset path, number of epochs, learning rate, validation split, and logging frequency.
[MODEL]	Selects the model architecture (e.g., ViT, EfficientNet), version, and pre-trained weights.
[EVAL]	Specifies the default directory path for the evaluation dataset.
[HF]	Stores settings for Hugging Face integration and model repository management.

The system generates results in user-friendly formats including console output for single files, `CSV` (Comma-separated Values) tables with Top-`N` predictions for batch processing, and confusion matrix plots for performance visualization. Cross-platform (Linux/Windows) scripts are provided for converting multi-page PDF documents into individual page images and for sorting annotated images into the required directory structure.

## 5 Results

This section details the practical integration of the classification systems into archival workflows and presents a comprehensive performance evaluation.

### 5.1 Integration into Archives

A primary objective was to develop a system that is not only accurate but also practical for use within existing archival processes.

#### 5.1.1 Deployment and Usability

The system has been packaged for local deployment under the MIT license, ensuring suitability for any institutional environment. It is designed for on-premises operation, an essential feature for archives managing sensitive or restricted collections. Standard `CPU` (Central Processing Unit) hardware suffices for inference, though a GPU is recommended for fine-tuning on user-annotated datasets and for accelerating large-batch inference.

The core functionality is platform-agnostic, compatible with both Linux and Windows operating systems. On a modern office desktop computer, the system can process several hundred thousand pages in under a week, with throughput potentially exceeding one million pages on higher-end hardware. For optimal performance utilizing Compute Unified Device Architecture (`CUDA`) for GPU acceleration, an NVIDIA graphics card is required. Users must allocate up to 30 GB disk space to accommodate Python dependencies, model weights, and datasets.

In a practical scenario, the classifier is integrated into the digitization pipeline: as documents are scanned, the tool assigns a classification label to each page, enabling efficient routing to subsequent processing stages — plain text to an OCR engine, tables to a structured data extraction module, and illustrations to specialized image analysis.

#### 5.1.2 Agreement with Field Experts

The system’s classification logic was refined based on criteria established in collaboration with archival experts. The final expert-validated criteria are as follows:

- All photographs or drawings of a significant size (at least postage-stamp sized) must be identified as `PHOTO` or `DRAW`, enabling targeted extraction of graphical content.

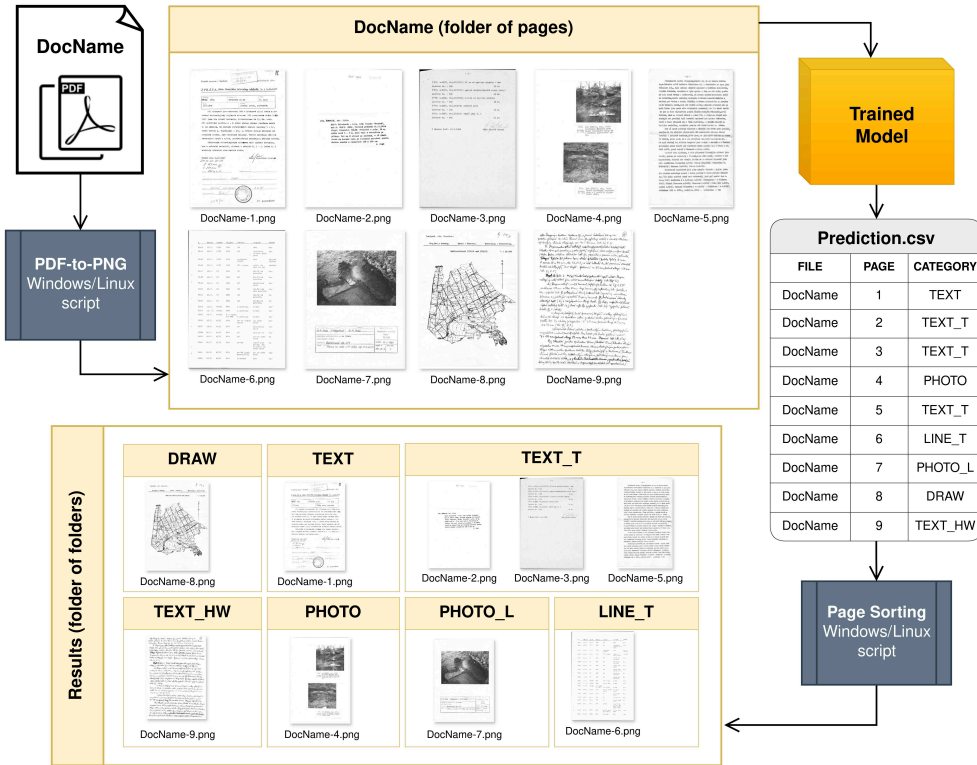


Fig. 13 Model inference use-case: processing a single PDF file into sorted and classified pages

- All tables and forms, regardless of border visibility, must be detected for subsequent structured data extraction, classified as `LINE_T`, `LINE_P`, or `LINE_HW`.
- Only pages containing clean, uniform text should be classified as `TEXT_T`, `TEXT_P`, or `TEXT_HW`. Minor elements such as handwritten page numbers may be ignored.
- Pages with mixed text styles, classified as `TEXT`, may include minor graphical elements such as newspaper logos. Extraction of these small elements is deemed unnecessary.
- Graphical elements within tabular layouts or accompanied by table-like legends must be classified as `PHOTO_L` or `DRAW_L`, signaling the need to extract both graphical content and structured data.

## 5.2 Accuracy Performance of Tested Models

A rigorous performance comparison was conducted across all evaluated architectures, measured by Top-1 accuracy on the 5,449-page held-out test set. The temporal distribution of this test

subset is shown in Fig. 14, confirming it covers the full chronological span of the archive. The results are presented in Table 7.

Table 7 demonstrates the following key findings:

- **RegNetY CNN:** RegNetY-16GF achieves the highest overall accuracy ( $\approx 99.16\%$ ) with a moderate parameter count (83.6 M) at  $224 \times 224$  resolution, outperforming the much larger 64GF variant (281.4 M). RegNetY-16GF is therefore the most efficient choice for production deployment. It also handles the dataset’s hardest distinction (`TEXT` vs. `TEXT_T`) best, reaching 94% accuracy on `TEXT` with only 5.1% confusion.
- **EfficientNet CNN:** EfficientNetV2-M achieves  $\approx 98.83\%$  with only 54.1 M parameters at  $384 \times 384$ . The smaller EfficientNetV2-S (48.2 M) remains a practical option for lower-resource machines. EfficientNetV2-L underperforms its smaller sibling, confirming that capacity scaling is not monotone on this task.
- **Vision Transformers:** ViT-large reaches  $\approx 99.12\%$  with 304.7 M parameters, nearly

**Fig. 14** Distribution of categories in the performance test subset (5,449 pages not included in any cross-validation training fold), based on document creation year. The test set covers the full chronological range of the archive

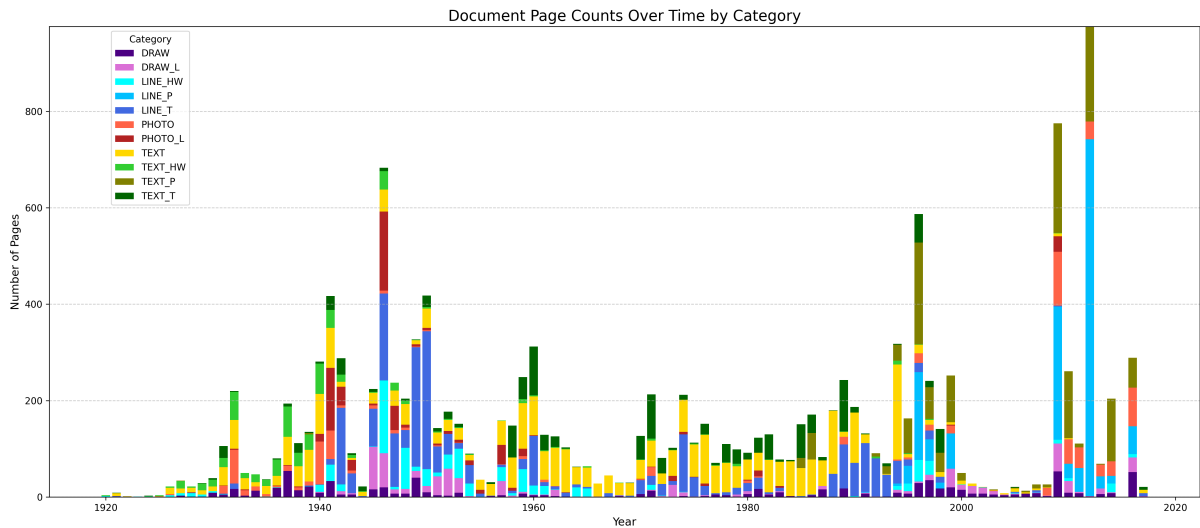
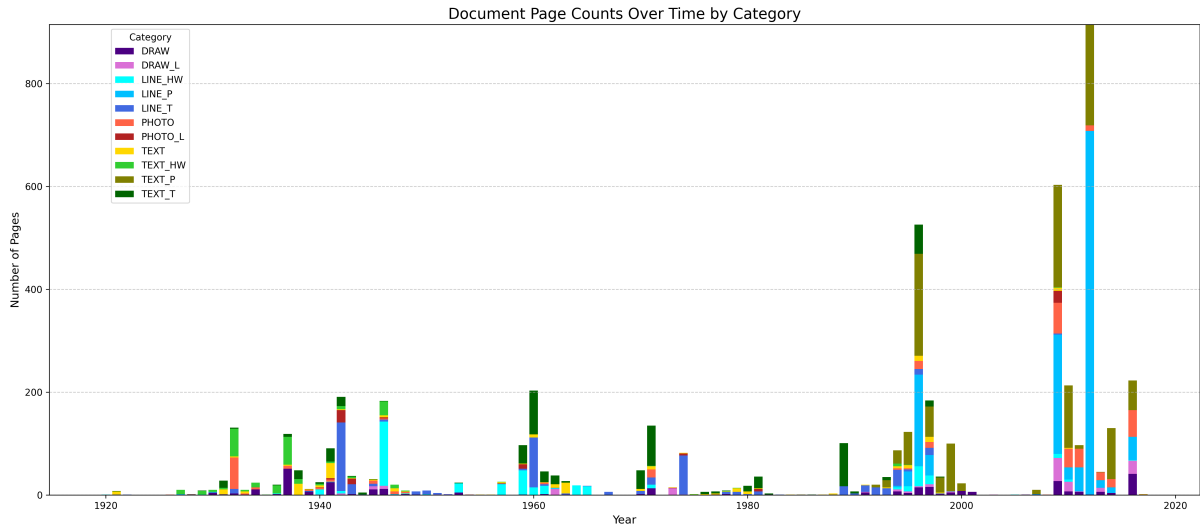


**Fig. 15** Category distribution in the expanded test dataset (all non-training samples from the first-fold split, random seed 420; 14,162 pages)

matching RegNetY-16GF at substantially higher computational cost. ViT-base at  $224 \times 224$  achieves 98.37% with only 86.6 M parameters.

- **Document Image Transformers:** DiT variants achieve 98–99% Top-1 accuracy. Despite pre-training on document images, they do not surpass the best CNNs or ViT-large at comparable parameter budgets.

- **CLIP Models:** In zero-shot mode, CLIP’s performance is inadequate for this domain ( $< 50\%$ ; confusion matrices in [4]). After 7 epochs of fine-tuning, the best CLIP configuration (ViT-B/16 with *mid* descriptions) achieves 99.14% — competitive with RegNetY-16GF. However, see Sect. 5.3 for an important caveat regarding CLIP’s real-world deployment behavior.

**Table 7** Comparison of Top-1 accuracy and model complexity for all evaluated architectures on the 5,449-page test set. *Italic*: most parameter-efficient per model family; **bold**: best-performing (above efficiency trendline) per family. CLIP results are from the *mid* description set for fine-tuned and averaged text features for zero-shot. Per-fold standard deviations and full confusion matrices are reported in [4]

Model	Parameters (M)	Input Size	Accuracy Top-1 (%)
<i>EfficientNet-v2-S</i>	<i>48.2</i>	<i>300×300</i>	<i>97.87</i>
<b>EfficientNet-v2-M</b>	<b>54.1</b>	<b>384×384</b>	<b>98.83</b>
EfficientNet-v2-L	118.5	384×384	98.62
<i>RegNetY-12GF</i>	<i>51.8</i>	<i>224×224</i>	<i>98.29</i>
<b>RegNetY-16GF</b>	<b>83.6</b>	<b>224×224</b>	<b>99.16</b>
RegNetY-64GF	281.4	384×384	98.79
<i>dit-base-rvldcip</i>	<i>86</i>	<i>224×224</i>	<i>98.26</i>
dit-large	304	224×224	97.91
<b>dit-large-rvldcip</b>	<b>304</b>	<b>224×224</b>	<b>98.53</b>
<i>vit-base-patch16</i>	<i>86.6</i>	<i>224×224</i>	<i>98.37</i>
vit-base-patch16	86.9	384×384	98.12
<b>vit-large-patch16</b>	<b>304.7</b>	<b>384×384</b>	<b>99.12</b>
<b>CLIP-ViT-B/16</b>	<b>150</b>	<b>224×224</b>	<b>99.14</b>
CLIP-ViT-B/32	151	224×224	98.99
CLIP-ViT-L/14	428	224×224	98.97
CLIP-ViT-L/14	428	336×336	98.97

Given the offline, batch-processing nature of archival workflows, the modest additional inference time for transformer-based models is acceptable. Balancing accuracy, model size, and consistency on unlabeled data, we selected **RegNetY-16GF (224)** as the primary deployment model, with **ViT-large-patch16 (384)** as a higher-resource alternative. CLIP-ViT-B/16 was released as a supplementary model for research use cases.

#### *On uncertainty and comparability.*

The accuracies in Table 7 for image-only models are reported on the single, fixed 5,449-page test set, which is disjoint from the training subset of every cross-validation fold; the deployed weights are the element-wise average of the five per-fold checkpoints, and the per-fold accuracies underlying each averaged model, together with their spread, are tabulated in [4]. Per-model Top-1 confusion matrices for every evaluated architecture, grouped by family, are provided as Online Resource 5, with full-resolution versions in [4]. The differences among the top image-only models (RegNetY-16GF, ViT-large, EfficientNetV2-M) are small and fall within the per-fold variation,

so we do not claim a statistically significant ranking among them; our deployment choice rests on the size–accuracy trade-off and, decisively, on the unlabeled-collection consistency analysis in Sect. 5.3. CLIP, by contrast, was fine-tuned on a single fold owing to its substantially higher training cost, so no cross-fold variance is available for it. Its 99.14% should therefore be read as a point estimate on one fold rather than a fold-averaged figure directly comparable to the image-only numbers; accordingly, our assessment of CLIP relies on its deployment behaviour (Sect. 5.3) rather than on this test-set score.

### 5.3 Prediction Agreement on the Unlabeled Collection

The accuracy comparisons in Sect. 5.2 are based on the 5,449-page annotated test set. To assess behavior on real-world archival data, we additionally applied the best image-only and CLIP-based models to the full unlabeled collection of 649,508 pages and measured pairwise agreement between their predictions.

As shown in Fig. 17, image-only models (EfficientNetV2-M, ViT-B/224, ViT-B/384,

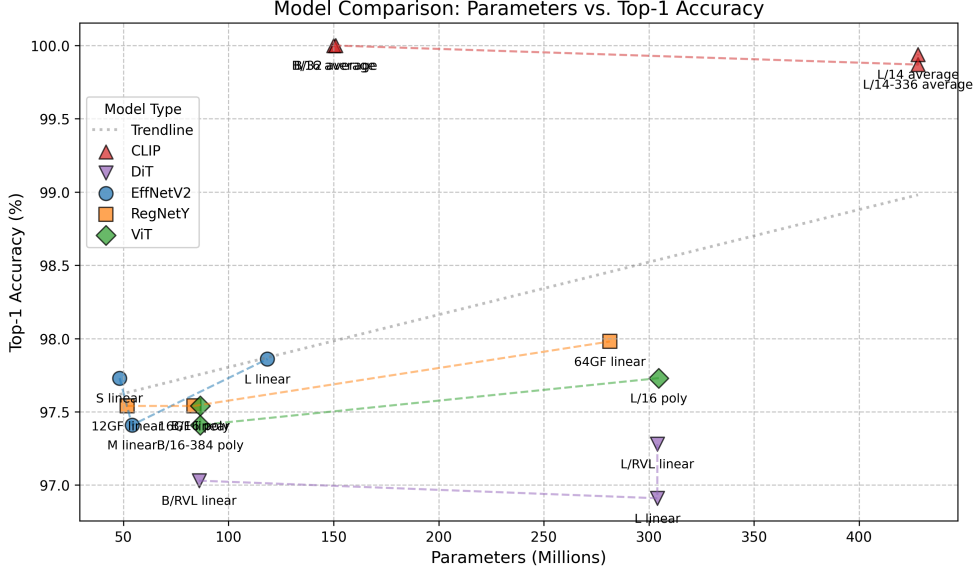


**Fig. 16** Accuracy vs. Parameter Count across evaluated models. Models above the trendline deliver superior efficiency. RegNetY-16GF and CLIP ViT-B/16 both sit above the trendline, while larger CLIP-L variants fall below it

RegNetY-16GF, ViT-large/384) share over 90% agreement in their per-page predictions. In contrast, CLIP variants agree with any image-only model at under 65%, and even disagree substantially among themselves (inter-CLIP agreement as low as 19% for different description sets).

The data providers confirmed that the low agreement of CLIP predictions makes automated archival labeling harder to trust: CLIP variants failed to assign a consistent category to over 80% of the unlabeled pages. One likely explanation is that CLIP overfits to annotated pages, inflating accuracy on the held-out test set while generalizing poorly to the full diversity of the collection. Another factor is that CLIP’s multimodal text prompts may be too ambiguous for categories such as DRAW, which merges maps, illustrations, and schematics under a single label.

Image-only models assign consistent labels across the entire archive and produce a plausible distribution aligning with archivists’ expectations. The dominant errors are concentrated in two well-understood confusions: TEXT vs. TEXT\_T (mixed vs. pure typed text) and DRAW vs. DRAW\_L. RegNetY-16GF performs best on both distinctions, reaching 94% accuracy on TEXT and 99% on DRAW.

We therefore released fine-tuned CLIP variants mainly for research and illustrative purposes. For operational archival management, image-only

architectures — and RegNetY-16GF in particular — are the recommended choice.

## 6 Conclusion

This work addressed the critical need for automated page-image classification in heterogeneous historical archives. After establishing the unique challenges of our dataset — visual defects, skew, and mixed content types (Sect. 4.1) — we demonstrated the shortcomings of off-the-shelf DLA tools and a lightweight RFC baseline, which achieved only  $\sim 75\%$  accuracy (Sect. 4.2.2). This aligns with broader surveys noting the limitations of hand-crafted features [7].

Fine-tuning modern CNNs (RegNetY and EfficientNetV2 families) markedly improved performance to  $\approx 97.9\text{--}99.2\%$ , with RegNetY-16GF achieving the top score of 99.16%. Fine-tuned ViT and DiT models consistently matched CNNs, with ViT-large reaching  $\approx 99.12\%$  Top-1 accuracy (Table 7).

CLIP models, once fine-tuned for 7 epochs, also achieved competitive test-set accuracy ( $\approx 99.14\%$  for the best configuration). However, a subsequent analysis on 649,508 unlabeled pages revealed that CLIP predictions diverge substantially from image-only models and show low inter-model consistency (Sect. 5.3), making them less

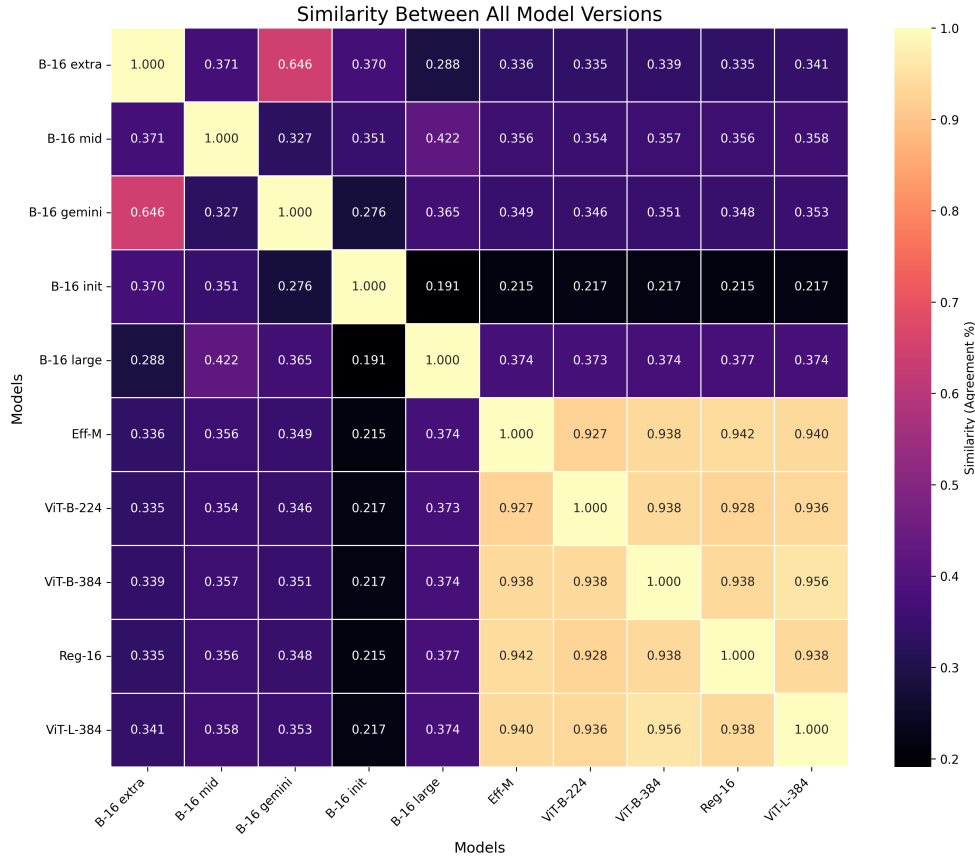


**Fig. 17** Pairwise prediction agreement between CLIP variants (first five rows/columns: B-16 with five description sets) and image-only models (last five rows/columns) applied to the full unlabeled collection of 649,508 pages. Image-only models share over 90% agreement; CLIP models agree with image-only models at under 65% and show low inter-CLIP consistency

suitable for large-scale archival sorting. Based on this comprehensive evaluation, **RegNetY-16GF (224)** was selected as the primary deployment model, with ViT-large-patch16 as a higher-resource alternative.

**Contributions:**

- Analyzed archival page-image characteristics and the failure modes of existing DLA tools.
- Established a resource-efficient RFC baseline creating a ~75% accuracy benchmark on the demo category sets.
- Built and released an annotated dataset of over 48,000 historical page images (Dataset 3), refined through four successive annotation stages with domain-expert review [27].
- Identified RegNetY-16GF as the primary deployment model by fine-tuning and comparing CNNs, Transformers, and multimodal architectures across five cross-validation folds.

- Demonstrated that image-only models produce substantially more consistent predictions on unlabeled archival data than fine-tuned CLIP variants — a finding with direct implications for deployment trust.
- Identified EfficientNetV2-M as the best accuracy/parameter trade-off among CNNs and ViT-large as the strongest Transformer alternative; all models above the accuracy–model-size efficiency trendline are released at [ufal/vit-historical-page](#) [26].
- Released fine-tuned CLIP model variations at [ufal/clip-historical-page](#) for research purposes.
- Provided deployment guidance for large-scale, on-premises archival processing, including a configurable pipeline and an extensible category taxonomy.
- Published the dataset [27] and software solution [26] in accordance with FAIR principles.

### Future Work:

- Explore further architectural optimizations for improved efficiency and performance.
- Integrate the classifier into broader digital archive management systems, noting its compatibility beyond archaeological archives.
- Expand the category taxonomy to include additional document types (e.g., Table 13).
- Incorporate larger datasets to enhance model generalization — work is already in progress at IAP.
- Develop finer-grained CLIP category descriptions (e.g. splitting DRAW into maps, schematics, and freehand sketches) to reduce multimodal model disagreement on unlabeled data.
- Facilitate later fine-tuning stages using predictions refined by users, enhancing system adaptability over time.
- Conduct a controlled dual-annotation study on a held-out subset to report a formal inter-annotator agreement ( $\kappa$ ) coefficient.

By delivering near-perfect classification accuracy, consistent real-world behavior, and a practical deployment framework, this research paves the way for significantly reduced manual effort in historical document workflows, supporting digital humanities research and mass digitization initiatives [1, 7].

## Statements and Declarations

**Funding.** The conducted research received funding from the European Commission HORIZON Research and Innovation Actions under grant agreement GAP-101132163 — **ATRIUM** — HORIZON-INFRA-2023-SERV-01-02 — **Advancing FrontTier Research In the Arts and hUManities**. Computing resources were provided by the Institute of Formal and Applied Linguistics (Ústav formální a aplikované lingvistiky (ÚFAL), **IFAL**), Charles University, via access to their CPU and GPU cluster nodes.

**Competing Interests.** The authors declare no competing interests.

**Author Contributions.** Kateryna Lutsai: conceptualization, data curation, software, experiments, formal analysis, writing (original draft). Pavel Straňák: supervision, project administration, review and editing. David Novák: project management, data provision, domain validation.

Dana Křivánková: domain expertise, annotation review, validation, review and editing. All authors read and approved the final manuscript.

**Data Availability.** The annotated dataset is publicly available at the LINDAT repository [27], containing more than 35 GB of source pages complemented with an annotation table of more than 48,000 images. The software is publicly available under the MIT license at [26]. Fine-tuned models are hosted on HuggingFace at [ufal/clip-historical-page](#) and [ufal/vit-historical-page](#).

## Acknowledgements

The project was managed by Mgr. David Novák, Ph.D. (IAP), whose coordination was instrumental throughout. The thesis on which this work is based was mentored by doc. RNDr. Pavel Pecina, Ph.D. (IFAL). The authors also thank the archivists of the Institutes of Archaeology in Prague and Brno for providing the source collection and for their feedback during annotation and validation.

## Supplementary Information

The following Online Resources are submitted as supplementary files accompanying this article:

**Online Resource 1** (ESM.1.pdf): Visual defect examples from the archive. Includes representative samples of grayish backgrounds, page skew, bleed-through, water damage, corner holes, edge holes, stamps, fat-journal curl, manual corrections, and mixed paper textures referenced throughout Sect. 3.1.1.

**Online Resource 2** (ESM.2.pdf): DeepDoc-tecture (DD) parsing attempts. Shows correct detections as well as failure modes on drawings, maps, photographs, tables, plain text, and newspaper layouts referenced in Sect. 4.1.

**Online Resource 3** (ESM.3.pdf): Category examples. Provides multiple representative scan examples (portrait and landscape orientation) for each of the 11 classification categories (DRAW, DRAW\_L, LINE\_HW, LINE\_P, LINE\_T, PHOTO, PHOTO\_L, TEXT, TEXT\_HW, TEXT\_P, TEXT\_T) referenced in Sect. 4.2.1 and Tables 1–3.

**Online Resource 4** (ESM.4.pdf): Dataset temporal distributions and cross-validation split proportions. Includes (a) stacked annual page counts per category across Dataset 0, Dataset 2,

and Dataset 3 annotation versions (showing the characteristic 1990s gap), and (b) category proportions in train, development, and test subsets across all five cross-validation folds plotted on a document-creation-date timescale.

**Online Resource 5** (ESM\_5.pdf): Per-model Top-1 confusion matrices on the 5,449-page test set, grouped by architecture family: RegNetY and EfficientNetV2 (CNNs), DiT and ViT (Transformers), and fine-tuned CLIP variants (averaged text features). Rows are true labels and columns predictions, normalized per row over the 11 categories, with each panel labelled by model variant and its Top-1 accuracy. Referenced in Sect. 5.2; full-resolution and zero-shot versions appear in [4].

## Use of AI Tools

This manuscript was prepared with the assistance of Large Language Models (LLMs). Drafts of individual sections were generated from author-supplied bullet points and factual outlines using Gemini 2.5 and GPT-4, then reviewed and post-edited by the authors to ensure factual accuracy. Grammarly and Writefull were used for grammar and style corrections. In all cases, the authors take full accountability for the final version of the text and confirm that the edits reflect our original work. This disclosure covers the generative use of AI tools; AI-assisted copy editing per se does not require declaration per Springer Nature guidelines.

## References

- [1] Nikolaidou, K., Seuret, M., Mokayed, H., Liwicki, M.: A survey of historical document image datasets. *International Journal on Document Analysis and Recognition (IJ DAR)* **25**(4), 305–338 (2022) <https://doi.org/10.1007/s10032-021-00390-6>
- [2] Zhong, X., Tang, J., Yepes, A.J.: PubLayNet: Largest dataset ever for document layout analysis. In: 2019 International Conference on Document Analysis and Recognition (ICDAR), pp. 1015–1022 (2019). <https://doi.org/10.1109/ICDAR.2019.00166> . IEEE
- [3] Xu, Y., Li, M., Cui, L., Huang, S., Wei, F., Zhou, M.: LayoutLM: Pre-training of text and layout for document image understanding. In: Proceedings of the 26th ACM SIGKDD International Conference on Knowledge Discovery & Data Mining, pp. 1192–1200 (2020). <https://doi.org/10.1145/3394486.3403172>
- [4] Lutsai, K., Straňák, P.: Page image classification for content-specific data processing (2026). <https://arxiv.org/abs/2507.21114>
- [5] Lewis, D.D., Agam, G., Argamon, S., Frieder, O., Grossman, D., Heard, J.: Building a test collection for complex document information processing. In: Proceedings of the 29th Annual International ACM SIGIR Conference on Research and Development in Information Retrieval, pp. 665–666 (2006). <https://doi.org/10.1145/1148170.1148307>
- [6] Harley, A.W., Ufkes, A., Derpanis, K.G.: Evaluation of deep convolutional nets for document image classification and retrieval. In: 2015 13th International Conference on Document Analysis and Recognition (ICDAR), pp. 991–995 (2015). <https://doi.org/10.1109/ICDAR.2015.7333910> . IEEE
- [7] Liu, L., Wang, Z., Qiu, T., Chen, Q., Lu, Y., Suen, C.Y.: Document image classification: Progress over two decades. *Neurocomputing* **453**, 223–240 (2021) <https://doi.org/10.1016/j.neucom.2021.05.003>
- [8] Tan, M., Le, Q.V.: EfficientNetV2: Smaller models and faster training. In: International Conference on Machine Learning (ICML), pp. 10096–10106 (2021). PMLR
- [9] Tan, M., Le, Q.: EfficientNet: Rethinking model scaling for convolutional neural networks. In: International Conference on Machine Learning (ICML), pp. 6105–6114 (2019). PMLR
- [10] Radosavovic, I., Kosaraju, R.P., Girshick, R., He, K., Dollár, P.: Designing network design spaces. In: Proceedings of the IEEE/CVF Conference on Computer Vision and Pattern Recognition (CVPR), pp. 10428–10436 (2020). <https://doi.org/10.1109/CVPR42600.2020.01044>

- [11] Dosovitskiy, A., Beyer, L., Kolesnikov, A., Weissenborn, D., Zhai, X., Unterthiner, T., Dehghani, M., Minderer, M., Heigold, G., Gelly, S., *et al.*: An image is worth 16x16 words: Transformers for image recognition at scale. In: International Conference on Learning Representations (ICLR) (2021). <https://openreview.net/forum?id=YicbFdNTTy>
- [12] Beyer, L., Zhai, X., Kolesnikov, A.: Better plain ViT baselines for ImageNet-1k. arXiv preprint arXiv:2205.01580 (2022)
- [13] Touvron, H., Cord, M., Douze, M., Massa, F., Sablayrolles, A., Jégou, H.: Training data-efficient image transformers & distillation through attention. In: International Conference on Machine Learning (ICML), pp. 10347–10357 (2021). PMLR
- [14] Ridnik, T., Ben-Baruch, E., Noy, A., Zelnik-Manor, L.: ImageNet-21K pretraining for the masses. arXiv preprint arXiv:2104.10972 (2021)
- [15] Li, J., Xu, Y., Lv, T., Cui, L., Zhang, C., Wei, F.: DiT: Self-supervised pre-training for document image transformer. In: Proceedings of the 30th ACM International Conference on Multimedia, pp. 3530–3539 (2022). <https://doi.org/10.1145/3503161.3547911>
- [16] Radford, A., Kim, J.W., Hallacy, C., Ramesh, A., Goh, G., Agarwal, S., Sastry, G., Askell, A., Mishkin, P., Clark, J., *et al.*: Learning transferable visual models from natural language supervision. In: International Conference on Machine Learning (ICML), pp. 8748–8763 (2021). PMLR
- [17] Xu, H., Xie, S., Tan, X.E., Huang, P.-Y., Howes, R., Sharma, V., Li, S.-W., Ghosh, G., Zettlemoyer, L., Feichtenhofer, C.: Demystifying CLIP data. arXiv preprint arXiv:2309.16671 (2023)
- [18] Biswas, B., Bhattacharya, U., Chaudhuri, B.B.: Document image skew detection and correction: A survey. IET Image Processing **17**(14), 3985–4006 (2023) <https://doi.org/10.1049/ipr2.12876>
- [19] Smith, R.: An overview of the Tesseract OCR engine. In: Ninth International Conference on Document Analysis and Recognition (ICDAR 2007), vol. 2, pp. 629–633 (2007). <https://doi.org/10.1109/ICDAR.2007.4376991> . IEEE
- [20] Breiman, L.: Random forests. Machine Learning **45**, 5–32 (2001) <https://doi.org/10.1023/A:1010933404324>
- [21] Yousefi, J.: Image binarization using otsu thresholding algorithm. Ontario, Canada: University of Guelph **10**, 9 (2011)
- [22] Hu, M.-K.: Visual pattern recognition by moment invariants. IRE Transactions on Information Theory **8**(2), 179–187 (1962) <https://doi.org/10.1109/TIT.1962.1057692>
- [23] Haralick, R.M., Shanmugam, K., Dinstein, I.: Textural features for image classification. IEEE Transactions on Systems, Man, and Cybernetics (6), 610–621 (1973) <https://doi.org/10.1109/TSMC.1973.4309314>
- [24] Paszke, A., Gross, S., Massa, F., Lerer, A., Bradbury, J., Chanan, G., Killeen, T., Lin, Z., Gimelshein, N., Antiga, L., *et al.*: PyTorch: An imperative style, high-performance deep learning library. In: Advances in Neural Information Processing Systems (NeurIPS), vol. 32 (2019)
- [25] Wolf, T., Debut, L., Sanh, V., Chaumond, J., Delangue, C., Moi, A., Cistac, P., Rault, T., Louf, R., Funtowicz, M., *et al.*: HuggingFace’s Transformers: State-of-the-art natural language processing. In: Proceedings of the 2020 Conference on Empirical Methods in Natural Language Processing (EMNLP): System Demonstrations, pp. 38–45 (2020). <https://doi.org/10.18653/v1/2020.emnlp-demos.6>
- [26] Lutsai, K., Stranak, P., Novak, D., Krivankova, D.: ATRIUM’s Page Classifier: Classification of Historical Page Images Using Fine-tuned ViT. <https://github.com/ufal/atrium-page-classification>
- [27] Lutsai, K., Krivankova, D.: Annotated Page Images from the (archaeological) Historical Archive. <http://hdl.handle.net/20.500>.

## Appendix A CLIP Category Descriptions

The full suite of eight category description sets used for CLIP fine-tuning and zero-shot evaluation is reproduced in the accompanying thesis [4]. Table 8 summarizes all sets; Tables 9 and 10 reproduce the two most referenced sets (*init* and *mid*) for convenience.

## Appendix B System Overview

The system’s primary entry point is the `run.py` script, which provides a comprehensive CLI for granular control over the system’s operations. The available flags are organized by user group, as shown in Table 11.

**Table 8** Summary of CLIP document classification description sets. “Rev.” denotes the revision fine-tuned to a specific label set of text features

Table Label	Summary
init 9	Provides the full “initial” set of classification categories with detailed distinctions between drawings, photos, and text, and further separates content by handwritten (HW), printed (P), and typed (T) forms both inside and outside tables or forms.
mid 10	Offers a more concise restatement of the initial taxonomy, trimming phrasing while preserving the same category distinctions, emphasizing brevity for quick reference.
min	Distills the taxonomy to its bare essentials, reducing each description to the minimal wording needed to convey whether an element is a drawing, table, photo, or text and its modality.
gpt	Reframes the classification around page-level context, explicitly noting that each label applies to an entire page containing the specified content (proposed by GPT-4 Deep Research).
short	Adapts the minimal set by omitting the word “page” and refining descriptions to emphasize cropped or cell-level occurrences.
gemini	Expands upon the page-based version with verbose, researcher-oriented descriptions, adding more examples and elaboration per category (proposed by Gemini 2.5 Deep Research).
extra	Presents a balanced yet thorough taxonomy enriched with illustrative examples.
detailed	Delivers the most detailed annotation-driven version, augmenting each label with notes on layout, annotation styles, and use-case examples.

**Table 9** Initial document classification labels (*init* set)

Label	Description
DRAW	drawings, maps, paintings, schematics, graphics with labels
DRAW_L	drawings, maps, paintings, schematics, graphics with a table legend, inside a table or form
LINE_HW	handwritten text lines inside a table or form
LINE_P	printed text lines inside a table or form
LINE_T	typed text lines inside a table or form
PHOTO	photos or cutouts from photos with labels
PHOTO_L	photos with a table caption, inside a table or form
TEXT	mixed printed and handwritten texts
TEXT_HW	handwritten text page
TEXT_P	printed text page
TEXT_T	typed document page

**Table 10** Short document classification labels (*mid* set) — the best-performing CLIP configuration

Label	Description
DRAW	a drawings or a map or a diagram
DRAW_L	a table and drawings or a map or a diagram
LINE_HW	a table or a filled form of handwritten texts
LINE_P	a table or a filled form of printed texts
LINE_T	a table or a filled form of typed texts
PHOTO	photos or photo cutouts
PHOTO_L	a table and photos or photo cutouts
TEXT	printed and handwritten text styles on a page
TEXT_HW	a handwritten plain text page or handwritten text paragraphs
TEXT_P	a printed plain text page or printed text paragraphs
TEXT_T	a typed plain text document page or typed text paragraphs

**Table 11** CLI options for `run.py`

Group	Flag	Alias	Description
<b>USER</b>			
	<code>--help</code>	<code>-h</code>	Displays available command options
	<code>--hf</code>		Interfaces with Hugging Face for model retrieval/publishing
	<code>--revision</code>	<code>-rev</code>	Specifies the model version
	<code>--model</code>	<code>-m</code>	Sets the base model architecture
	<code>--file</code>	<code>-f</code>	Processes a single image file
	<code>--directory</code>	<code>-d</code>	Explicitly specifies an input directory
	<code>--dir</code>		Uses the default directory from the configuration file
	<code>--topn</code>	<code>-tn</code>	Defines the number of top-N guesses to return
	<code>--raw</code>		Generates raw probability distributions for predictions
	<code>--batch_size</code>		Sets the batch size for training, evaluation, and inference
<b>CLIP-specific</b>			
	<code>--avg</code>		Uses an average of text features from all category descriptions
	<code>--model_path</code>		Specifies the filename of a local <code>.pt</code> model checkpoint
<b>DEV</b>			
	<code>--train</code>		Initiates a model training session
	<code>--eval</code>		Performs model evaluation on a dataset
	<code>--lr</code>		Sets the learning rate for training
	<code>--epochs</code>		Sets the number of epochs for training
	<code>--max_categ</code>	<code>-mc</code>	Sets the maximum samples per category for a training subset
	<code>--max_categ_eval</code>	<code>-mce</code>	Sets the maximum limit of samples per category for evaluation
	<code>--model_dir</code>		Specifies path to a directory of saved model checkpoints
	<code>--eval_dir</code>		Evaluates a directory of saved models

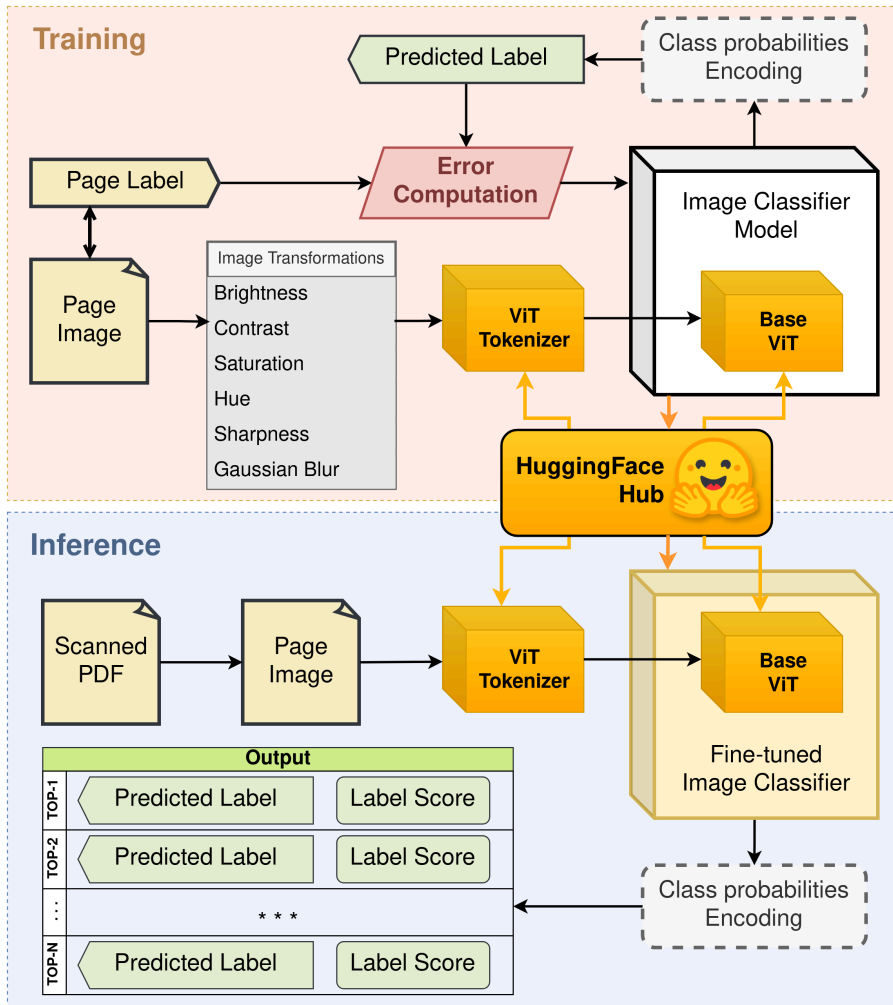


Fig. 18 Scheme of the Transformers and CNNs model architecture

	Printed	Typewritten	HandWritten	Mixed
Photos	<b>PHOTO</b>			
Drawings etc.	<b>DRAW</b>			
Photo in table	<b>PHOTO_L</b>			
Drawing in table	<b>DRAW_L</b>			
Tables & Forms	<b>LINE_P</b>	<b>LINE_T</b>	<b>LINE_HW</b>	
Plain texts	<b>TEXT_P</b>	<b>TEXT_T</b>	<b>TEXT_HW</b>	<b>TEXT</b>

Table 12 Defined labels coverage of the data features variability

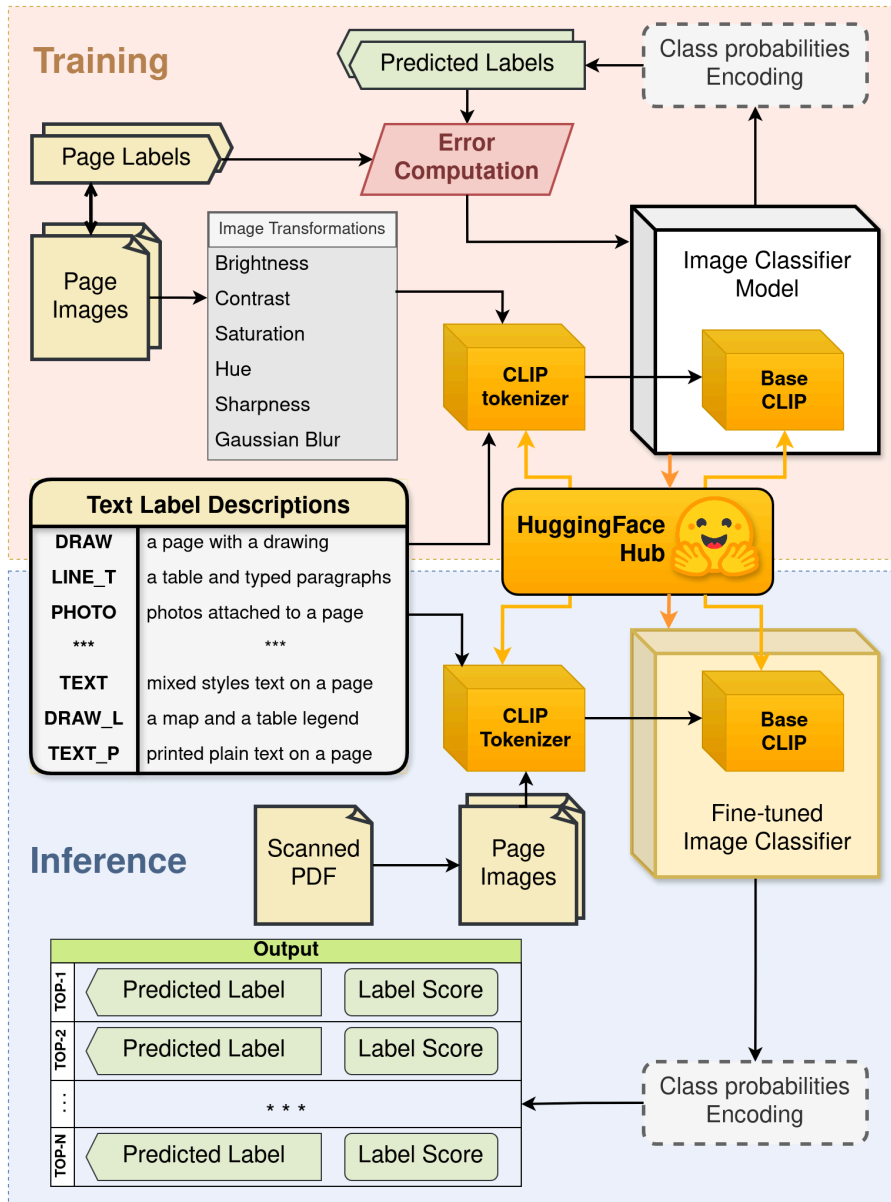


Fig. 19 Scheme of the CLIP model architecture

	Printed	Typewritten	Handwritten	Mixed
Photos	P_P	P_T	P_HW	PHOTO
Drawings	D_P	D_T	D_HW	DRAW
Photos in table	P_L_P	P_L_T	P_L_HW	PHOTO_L
Drawings in table	D_L_P	D_L_T	D_L_HW	DRAW_L
Tables & Forms	LINE_P	LINE_T	LINE_HW	LINE
Plain texts	TEXT_P	TEXT_T	TEXT_HW	TEXT

Table 13 Expanded labels coverage of the data features variability